Natural Motion Generation of Proactive Human Interface PICO-2

Ryo Kurazume Tsutomu Hasegawa

Graduate School of Information Science and Electrical Engineering
Kyushi University
6-10-1, Hakozaki, Higashi-ku, Fukuoka, 912-8581, JAPAN

Abstract

We are conducting research on "Embodied Proactive Human Interface". The aim of this research is to develop a new human-friendly active interface based on a new driving mechanism named "Proactive Interface" and a physical device using robot technology. This paper presents a new methodology for generating human-like natural motion of the humanoid-type proactive interface robot named PICO-2. For a variety of human motion, we focus on walking motion of PICO-2, and propose a new straight legged walking utilizing up-and-down motion of an upper body. Firstly, we define two new indexes, the Knee Stretch Index (KSI) and the Knee Torque Index (KTI), which indicate how efficiently the knee joints are utilized. Next, up-and-down motion of the upper body is automatically planned so that these indexes are optimized and straight legged walking is realized. The effectiveness of the proposed method is demonstrated by computer simulation and walking experiments using PICO-2.

1. Introduction

We are now conducting research on "Embodied Proactive Human Interface". The aim of this research is to develop a new human-friendly active interface based on a new driving mechanism named "Proactive Interface" and a physical device using robot technology. Figure 1 and Table 1 show the prototype of proactive human interface robot named PICO-2. This robot has two legs (6 dofs) and two arms (4 dofs + 1 dof for opening and closing fingers). A single CCD camera, a liquid crystal display, a microphone and a speaker are equipped on the head.

Table 1: Specification of PICO-2

Height	640 [mm]
Weight	8.7 [Kg]
Number of actuators	23

For a robot which is used as proactive human interface, it is important to perform human-like motion to avoid making uncomfortable feeling for users. However, conventional motion of a humanoid robot is generally unnatural [1]-[2]. For example, if we compare walking patterns of a human being and a biped robot, we will find the following differences: A human being utilizes up-and-down motion of an upper body or roll motion using a waist joint, knee joints, and ankle joints simultaneously. Instead, a conventional biped robot seems to walk very carefully by lowering its waist position and bending knee joints.

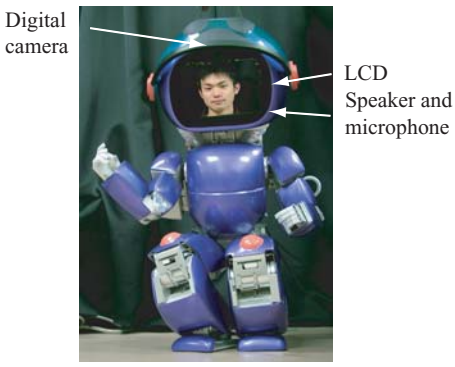

Figure 1: Proactive Human Interface Robot, PICO-2

The main reasons for this unnatural motion of a humanoid robot are as follows;

1. Mechanical factors
   (a) Different configuration of DOFs (Degree-of-freedoms)
   (b) Limited range of joint motion
2. Control factors
   (a) Uniformity of motion
   (b) Constraints related to control algorithms, for instance, singularity avoidance

This paper mainly discusses the control algorithm of a biped robot for generating natural walking pattern.

In general, most biped robots developed so far walk stably by bending their knee joints (Fig.3(a)). This is due to

the fact that controlling the Zero Moment Point (ZMP) becomes quite difficult when the knee joint is stretched and the some DOFs of motion are degenerated. On the other hand, human utilizes rotation of the waist joint and up-and-down motion of the upper body to secure the enough DOFs for stable walking. Fig.2 shows an example of a human walking pattern measured by motion capture system.

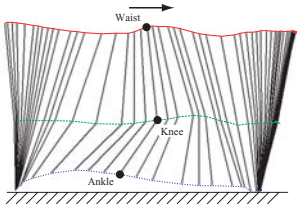

Figure 2: Up-down motion of waist position while walking

This paper presents a new methodology for generating a straight legged walking pattern for a biped robot utilizing up-and-down motion of an upper body (Fig.3(b)) [3]. Firstly, we propose two new indexes, the Knee Stretch Index (KSI) and the Knee Torque Index (KTI) for evaluating the efficiency of the use of the knee joints quantitatively, The Knee Stretch Index (KSI) is defined as the length between the line connecting the center of gravity (COG) and the ZMP, and the knee rotation axis. The Knee Torque Index (KTI) is also defined as the length between the ZMP on a knee plane and the knee rotation axis.

Next, the sway compensation trajectory [4] is modified so that up-and-down motion is automatically planned to optimize these indexes and straight legged walking is realized. The basic idea of the proposed method is as follows: i) when a number of DOFs of motion are required for precious control of the ZMP, a robot makes his body height lower to secure the enough DOFs, ii) when there is a extra number of DOFs of motion, the body is lifted and the knee joint is stretched in the same way as a walking pattern of human.

A few studies on straight legged walking have been reported so far. Recently, the Robo GARAGE, which is a venture company in Japan, announced a new humanoid-type robot named CHROINO [5]. This robot is able to walk stably with stretching knee joints by devising joint configuration.

The research group at Waseda University in Japan reported straight legged walking of a biped robot using their humanoid-type robot named WABIAN-2 [6], [7]. They adopted different algorithms for the calculation of inverse kinematics in supporting and recovering phases. The singularity is avoided by utilizing the roll motion of the waist joint.

Our method realizes the straight legged walking by controlling the height of the COG trajectory according to the state of the ZMP controller. The singularity is avoided by bending the knee joints when the ZMP has to be controlled precisely. On the other hand, the knee joints are stretched if the desired ZMP is almost attained and there is no need to control the ZMP position so precisely.

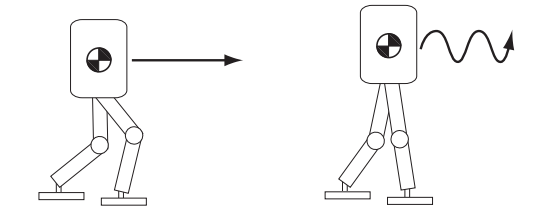

Figure 3: Height control during walking

There are several advantages for the straight legged and waist-lifted walking. Some of them are as follows;

1. Human-like natural walking motion is obtained
2. Energy efficiency is improved since required torque and energy consumption to support the body weight become small at knee joints.

2. The sway compensation trajectory for biped robots

In this section, the sway compensation trajectory for biped robots is introduced [4]. The ZMP and the COG trajectories are obtained by explicit functions of a sway width, a walking speed, acceleration and lines connecting the center of the soles of support feet.

2.1. Definition of the sway compensation trajectory

In the following discussion, we assume the weight of legs and arms are smaller than the body weight. In this case, the system can be regarded as a single mass model placed on (x_g, y_g, z_g)

Assuming a floor is flat and the height of the point mass z_g is constant, the ZMP on the floor $(x_{zmp}, y_{zmp}, 0)$ is obtained as follows:

$$\begin{pmatrix} x_{zmp} \\ y_{zmp} \end{pmatrix} = \begin{pmatrix} x_g \\ y_g \end{pmatrix} - A \begin{pmatrix} \ddot{x_g} \\ \ddot{y_g} \end{pmatrix} \quad (1)$$

where, $A = \frac{z_g}{g}$. Next, the diagonal line connecting the center of the soles of support feet is defined as

$$x \cos\theta + y \sin\theta = d \quad (2)$$

Then, in order to keep the ZMP on this line, the COG has to satisfy the following equation.

$$\cos\theta(x_g - A\ddot{x_g}) + \sin\theta(y_g - A\ddot{y_g}) = d \quad (3)$$

Here, we assume that the robot moves along x axis and the position of the body is expressed as

$$x_g = C_1^x e^{\frac{t}{\sqrt{A}}} + C_2^x e^{-\frac{t}{\sqrt{A}}} + a_2^x t^2 + a_1^x t + a_0^x \quad (4)$$

$$y_g = C_1^y e^{\frac{t}{\sqrt{A}}} + C_2^y e^{-\frac{t}{\sqrt{A}}} + a_2^y t^2 + a_1^y t + a_0^y \quad (5)$$

Eqs.(4) and (5) consists of a particular solution and a general solution of equations, $x_g - A\ddot{x_g} = 0$ and $y_g - A\ddot{y_g} = 0$. By substituting these equations into Eq.(3), we obtain

$$\cos\theta(a_0^x - 2Aa_2^x + a_1^x t + a_2^x t^2)$$
$$+ \sin\theta(a_0^y - 2Aa_2^y + a_1^y t + a_2^y t^2) = d \quad (6)$$

From Eq.(6) and the boundary condition, all the parameters such as a_0^x are determined [4]. The trajectory expressed by Eqs.(4) and (5) is named "the sway compensation trajectory".

Fig.4 shows an example of the ZMP and the COG trajectories in case that the robot walks 10 steps with the velocity $0.1m/s$ along the x axis from the initial position $(0, 0)$.

It should be pointed out that obtained trajectories can be easily modified and utilized if the moving direction is gradually changed. This is because continuous ZMP and COG trajectories are obtained by applying simple coordinate transformation to original trajectories according to the moving direction.

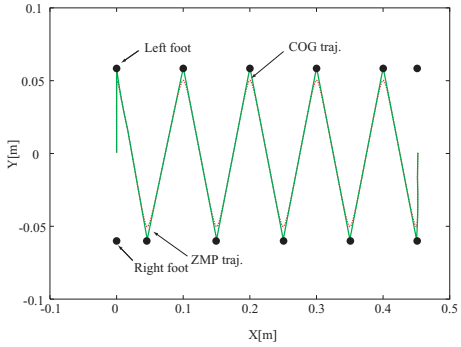

Figure 4: An example of ZMP and COG trajectories projected on the ground for straight path

2.2. Convergent calculation considering multiple mass model

The trajectories obtained as Eqs.(4) and (5) are based on the assumption of a simple single mass model. Therefore, more precise trajectories and joint commands should be determined based on a multiple mass model for stable walk. To obtain the precious ZMP trajectory based on the multiple mass model, we proposed the method which utilizes convergence calculation for rectifying the COG trajectory according to the current ZMP errors.

Firstly, the ZMP $X_{zmp} = (x_{zmp}, y_{zmp}, 0)$ for a multiple mass model is obtained from the following equations.

$$x_{zmp} = \frac{\sum_{i=1}^{N} m_i(r_{ix}(\ddot{r}_{iz} + g) - r_{iz}\ddot{r}_{ix}) - I_i\dot{\omega}_{iy}}{\sum_{i=1}^{N} m_i(\ddot{r}_{iz} + g)} \quad (7)$$

$$y_{zmp} = -\frac{\sum_{i=1}^{N} m_i(-r_{iy}(\ddot{r}_{iz} + g) + r_{iz}\ddot{r}_{iy}) - I_i\dot{\omega}_{ix}}{\sum_{i=1}^{N} m_i(\ddot{r}_{iz} + g)} \quad (8)$$

Here, we define the planned ZMP trajectory as X_{zmp}^{ref}, the refined COG trajectory to realize the planned ZMP trajectory as X_g^{ref}, and the current COG trajectory as X_g. Then, current status can be expressed as

$$X_{zmp} = X_g - A\ddot{X}_g \quad (9)$$

On the other hand, the goal status is shown as

$$X_{zmp}^{ref} = X_g^{ref} - A\ddot{X}_g^{ref} \quad (10)$$

Thus, by subtracting above equations, we obtain

$$X_{zmp}^{ref} - X_{zmp} = X_g^{ref} - X_g - A(\ddot{X}_g^{ref} - \ddot{X}_g) \quad (11)$$

or,

$$e_{zmp} = e_g - A\ddot{e}_g \quad (12)$$

where, $e_{zmp} = X_{zmp}^{ref} - X_{zmp}$, and $e_g = X_g^{ref} - X_g$. By resampling this equation with sampling interval Δt, the following equation is obtained.

$$\begin{aligned} e_{zmp}^t &= e_g^t - A\ddot{e}_g^t \\ &= e_g^t - A\frac{e_g^{t+1} - 2e_g^t + e_g^{t-1}}{(\Delta t)^2} \end{aligned} \quad (13)$$

Therefore, the rectified value of the COG trajectory e_g^t that reduces the ZMP error e_{zmp}^t is obtained as the following equation.

$$e_g^t = \frac{e_{zmp}^t + \frac{A}{(\Delta t)^2}(e_g^{t+1} + e_g^{t-1})}{1 + 2\frac{A}{(\Delta t)^2}} \quad (14)$$

However, several experiments showed that the refined COG trajectory tends to be oscillational at discontinuous point of the ZMP velocity, if the rectified value obtained from above equation is added directly to the original COG trajectory. Therefore, we choose the rectified value of the COG trajectory e_g^t so that the following equation with the smoothness constraint is minimized.

$$\min_{e_g^t}(e_g^t - \frac{e_{zmp}^t + \frac{A}{(\Delta t)^2}(e_g^{t+1} + e_g^{t-1})}{1 + 2\frac{A}{(\Delta t)^2}})^2 +$$
$$k(e_g^t + X_g^t - \frac{e_g^{t+1} + X_g^{t+1} + e_g^{t-1} + X_g^{t-1}}{2})^2 \quad (15)$$

Consequently, the refined COG trajectory that realizes the planned ZMP trajectory is obtained as the sum of the current COG trajectory X_g and the rectified value e_g^t.

$$X_g^{ref} \leftarrow X_g + e_g^t \tag{16}$$

In practice, considering the resampling error and non linearity of Eqs.(9) and (10), the above calculation should be repeated until e_g^t becomes sufficiently small value.

In summary, the proposed method which consists of two convergent calculation loops is described as follows;

1. The ideal ZMP trajectory X_{zmp}^{ref} is designed from Eqs.(1), (4), and (5). Then the COG trajectory X_g^0 that realizes the ideal ZMP trajectory is obtained approximately using a single mass model.
2. The trajectory of the reference position (ex. the waist position) and the joint trajectories of arms and legs Φ^n are calculated from the current COG trajectory X_g^n. Note that the tip trajectories of hands and legs are determined beforehand, and there is no change before and after the convergent calculation.
3. The actual ZMP trajectory based on the multiple mass model X_{zmp} is calculated using Eqs.(7) and (8) and the joint trajectories Φ^n.
4. The error between the ideal and the actual ZMP trajectories $e_{zmp} = X_{zmp}^{ref} - X_{zmp}$ is obtained. This error is discretized and the error at each time step e_{zmp}^t is calculated.
5. The rectification of COG trajectory e_g^t that minimizes Eq.(15) is calculated using the convergence calculation for all discretized error **(The first loop)**.
6. The refined COG trajectory $X_g^{n+1} = X_g^{ref}$ is obtained using Eq.(16).
7. The calculation is terminated if the sum of the rectification of COG trajectory e_g^t is small enough.
8. Go to Stop (2) **(The second loop)**

3. Knee Stretch Index and Knee Torque Index

The sway compensation trajectory is derived for a robot which can change the COG position at will. Thus, the knee joint has to be bent sufficiently to ensure enough DOFs of motion. However, by stretching the knee joints and keeping waist position high, several advantages can be considered as mentioned above. Especially, if the torque produced at the knee joint is reduced, it is quite useful in practical design since a small and light weight actuator.

However, no index has been proposed so far for indicating how much the knee joints utilized efficiently. For evaluating the efficiency of the use of the knee joints quantitatively, we propose two new indexes, the Knee Stretch Index (KSI) and the Knee Torque Index (KTI) in this section. Both indexes indicate the required torque at the knee joints to support the body weight with a simple calculation. Thus, it is possible to evaluate the efficiency of walking patterns using these indexes without a precise calculation of joint torque.

3.1. Knee Stretch Index

At first, we define the Knee Stretch Index (KSI). The KSI reflects the knee torque to support the body weight under the assumption of the single mass model.

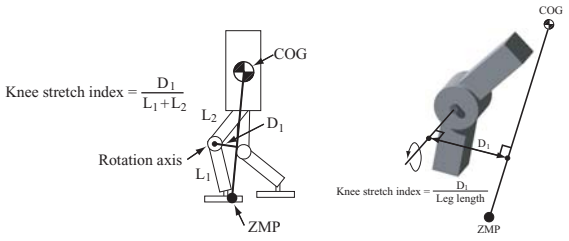

Figure 5: Definition of Knee Stretch Index

Fig.5 illustrates the definition of the Knee Stretch Index. If we assume that all the mass of the robot body is concentrated at the COG and the moment around the COG is negligible, the reactive force from the ground is exerted at the ZMP on the sole along the direction from the ZMP to the COG. Therefore, the torque to support the body weight at the knee joint is proportional to the distance from this line to the rotation axis of the knee joint. For example, in the case that the rotation axis of the knee joint is on the line between the COG and the ZMP, all the body weight is supported mechanically and there is no need to produce the torque at the knee joint.

From the above consideration, the Knee Stretch Index (KSI) is defined as a ratio of the minimum length D_1 between the line connecting the COG and the ZMP, and the leg length L, that is,

$$Knee\ Stretch\ Index = \frac{D_1}{L} \tag{17}$$

3.2. Knee Torque Index

Next, as a new index to evaluate the efficiency of the use of the knee joints more rigorously, we propose the Knee Torque Index (KTI). Imagine a plane which includes the representative point on the rotation axis at the knee joint and is parallel to ground. The representative point can be a point where, for example, the rotation axis intersects with

the center line of the leg. Then, the ZMP on this plane can be defined in the same manner as the conventional ZMP on the ground, and we call this ZMP the knee-plane ZMP (KZMP). Since no moment along roll and pitch axes exists at this KZMP, if this KZMP is on the rotation axis of the knee axis, no torque is required at the knee joint to support the body weight. Therefore, we define the Knee Torque Index (KTI) as a ratio of the length D_2 between the KZMP and knee rotation axis, and the leg length L such as

$$Knee\ Torque\ Index = \frac{D_2}{L} \tag{18}$$

Fig.6 indicates the definition of the Knee Torque Index (KTI). This KTI almost coincides with the KSI if the rotation axis of the knee joint is parallel to the ground and the moment around the COG is small.

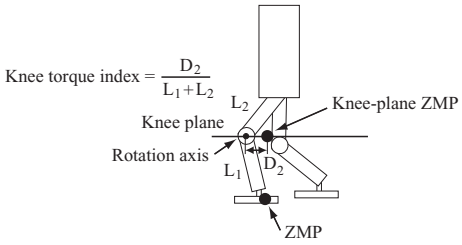

Figure 6: Definition of Knee Torque Index

4. New straight legged walking pattern

In this section, we propose a new straight legged walking pattern by controlling the height of the COG trajectory according to the state of the ZMP controller.

The sway compensation trajectory described in section 2 assumes the constant height of the waist position. In order to obtain the adaptive waist trajectory such as, i) when a large number of DOFs of motion are required for precious control of the ZMP, a robot makes its body height lower to secure the enough DOFs, ii) when there is a extra number of DOFs of motion, the body is lifted so that the index proposed in the previous section is minimized and the knee joint is stretched, we modify the steps 4 of the procedure of the sway compensation trajectory as follows:

4. The error between the ideal and the actual ZMP trajectories $e_{zmp} = X^{ref}_{zmp} - X_{zmp}$ is obtained. This error is discretized and the error at each time step e^t_{zmp} is calculated. In addition, when the knee joint angle is not 180 degrees (bending), the waist position is modified as $e^t_g \rightarrow e^t_g + \Delta P_{min}$. Here, ΔP_{min} is derived as follows: i) the COG position is moved slightly to new positions on a small circle around the current COG position in x-z plane (Fig.7), ii) the KSI (or the KTI) is calculated at each position and the position where the index is minimized is selected as ΔP_{min}.

   Contrary to this, when the knee joint angle is already 180 degrees and the ZMP error is larger than the predefined constant value as $e^t_{zmp} > e_{th}$, the waist position is lowered as $e^t_z \rightarrow e^t_z - \Delta H$. Actually, we use the smoothness constraint for e^t_z in the same way as Eq.(15).

$$\min_{e^t_z}(e^t_z - \Delta H)^2 + k(e^t_z + X^t_z - \frac{e^{t+1}_z + X^{t+1}_z + e^{t-1}_z + X^{t-1}_z}{2})^2 \tag{19}$$

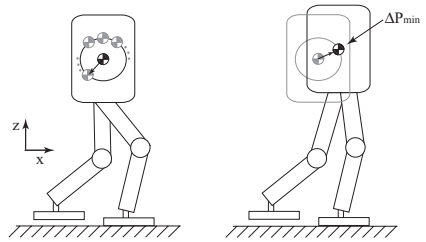

Figure 7: Calculation of ΔP_{min}

As a consequence of the above procedure, the robot makes its waist position lower if the knee joint is stretched and the some DOFs of motion are degenerated even if the ZMP error is large. On the other hand, the waist position is lifted and the KSI and/or the KTI are improved if the ZMP error is small and some DOFs of motion is redundant.

Furthermore, the solution of inverse kinematics cannot be obtained when the knee joint is completely stretched in general. Thus, our method adopts an approximated solution. Let's consider the case shown in Fig.8. Generally, the joint angle of the knee joint θ_4 is obtained using the cosine formula as

$$\theta_4 = \pi - \cos^{-1}\frac{L_1^2 + L_2^2 - l^2}{2L_1L_2} \tag{20}$$

Where L_1 and L_2 are the length of the thigh and shank, and l is the length between the ankle and the groin. However, the solution of the Eq.(20) cannot be obtained if $L_1 + L_2 < l$. Therefore, we use the following solution in this case as

$$\theta_4 = \begin{cases} \pi - \cos^{-1}\frac{L_1^2+L_2^2-l^2}{2L_1L_2} & (L_1 + L_2 \geq l) \\ \pi & (otherwise) \end{cases} \tag{21}$$

At the singular point where the knee joint is stretched, huge angular velocity is produced in case that the waist position is forced to be lowered. In our implementation, we defined the maximum and minimum values of the angular

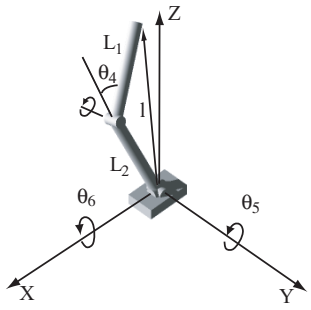

Figure 8: Approximated calculation of Inverse Kinematics

acceleration at the knee joint to avoid such case. By introducing this procedure at the step 2 in the above convergent calculation, the joint angle trajectory that minimizes the ZMP error is obtained under the constraint of the feasible angular velocity.

5. Experiments

This section introduces some examples of the proposed straight legged walking pattern though computer simulations and walking experiments using the humanoid-type proactive interface robot named PICO-2.

5.1. Computer simulation

Figs.9 and 10 show examples of the obtained walking patterns using the method proposed in Section III. Here, Fig.9 illustrates a conventional walking pattern which keeps the low waist position and bends the knee joints. Fig.10 is an obtained walking pattern after the convergent calculation using the proposed method. In these simulations, the walking period is 4 [sec.] and the maximum angular acceleration is set to $500[rad./sec.^2]$.

Fig.11 shows the change of the waist height before and after the convergent calculation. It is clear that the periodical up-and-down motion of the waist position is obtained gradually through the convergent calculation.

The joint angle of the knee joint is also shown in Fig.12. The lower figure of Fig.12 shows the joint trajectory during one supporting phase. After convergent calculation, the joint angle of the knee joint becomes about 180 degrees twice in one walking cycle.

Fig.13 shows the ZMP trajectories before and after convergent calculation. From this, it is verified that the ZMP error after the convergent calculation becomes smaller than the error without the convergent calculation even if up-and-down motion of the waist position exists and Eq.(1) is not satisfied.

Fig.14 and Table 2 show the total power consumption and the energy consumption in one walking cycle. The sum of the energy consumption of all actuators is 11.9[J] for

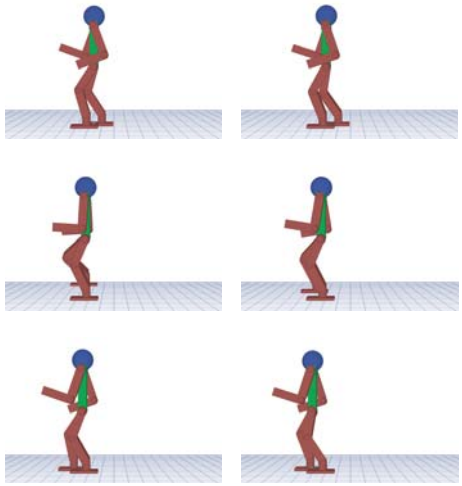

Figure 9: Conventional walking pattern

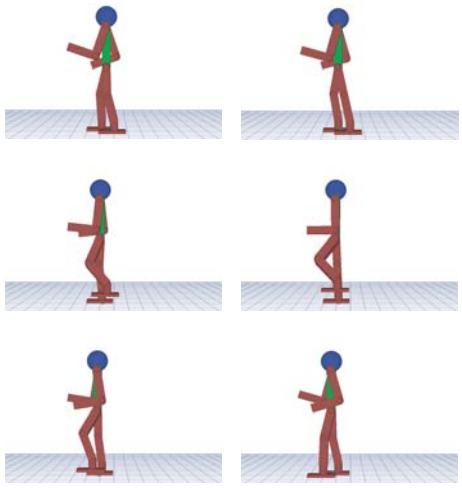

Figure 10: Obtained walking pattern after 100 iterations

the conventional walking pattern (Fig.9) and 7.6 [J] for the proposed walking pattern (Fig.10), respectively. Thus, it is clear that the proposed straight legged walking is more effective than the walking pattern which bends the knee joint in views of the energy consumption.

Finally, the proposed Knee Stretch Index and the Knee Torque Index for the obtained trajectories are shown in Figs.15 and 16. It is clear that both the KSI and the KTI for the proposed straight legged walking pattern becomes smaller than the ones for the conventional walking pattern. This means that the body weight is supported with small joint torque using the obtained straight legged walking pattern. Fig.17 shows the calculated joint torque at the knee joint of the right leg. The absolute value of the joint torque becomes small as expected from the KSI and the KTI if the proposed straight legged walking pattern is used. From these results, it is verified that the efficiency of walking pat-

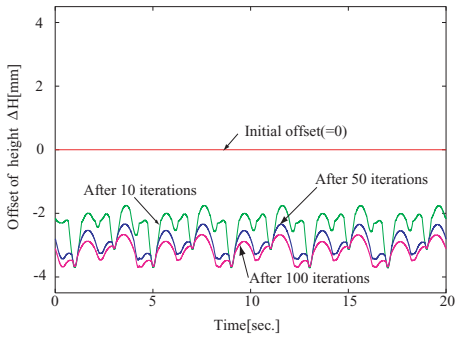

Figure 11: Height regulation by convergent calculation

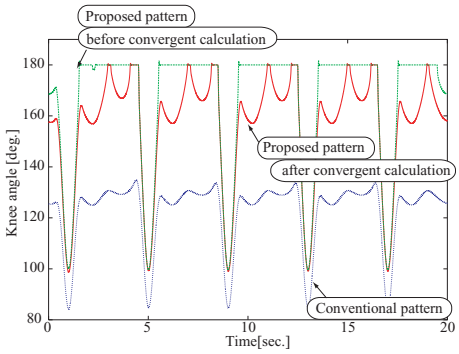

Figure 12: Knee joint angle

terns can be evaluated using these indexes instead of calculating precise joint torque.

5.2. Experiments using PICO-2

Walking experiments using the Humanoid-type proactive interface robot, PICO-2 were carried out. Figs.18 and 19 show the conventional and the proposed walking patterns of PICO-2. From these experiments, it is verified that the robot walks stably using the proposed straight legged walking pattern even when the robot stretches the knee joints.

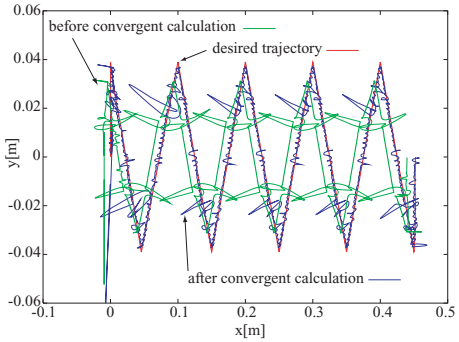

Figure 13: ZMP trajectory before and after convergent calculation

Table 2: Energy consumption in one walking cycle

Walking pattern	Energy consumption
Conventional pattern (Fig.9)	13.3 [J]
Proposed pattern (Fig.10)	6.5 [J]

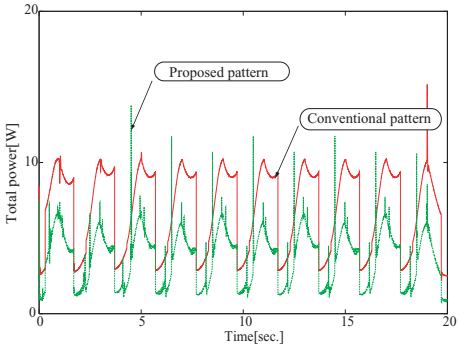

Figure 14: Total power consumption

6. Conclusions

This paper presents a new methodology for generating a straight legged walking pattern for the humanoid-type proactive interface robot named PICO-2. The advantages of the straight legged and waist-lifted walking are as follows:

1. Human-like natural walking motion is obtained
2. Required torque and energy consumption to support the body weight become small by stretching the knee joints

Two new indexes which evaluate how efficiently the knee joints are utilized, that is, the Knee Stretch Index (KSI) and Knee Torque Index (KTI), are proposed. Both indexes indicate the efficiency of the use of the knee joints quantitatively for the straight legged walking with a simple calculation. Up-and-down motion of the upper body is automatically planned so that these indexes are optimized and the straight legged walking is realized.

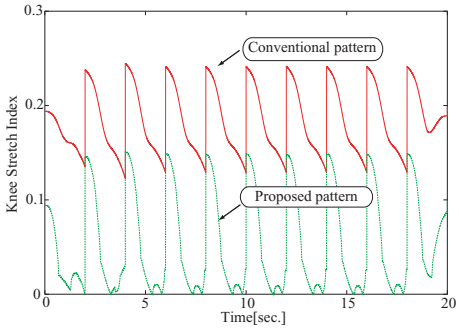

Figure 15: Comparison of Knee Stretch Index

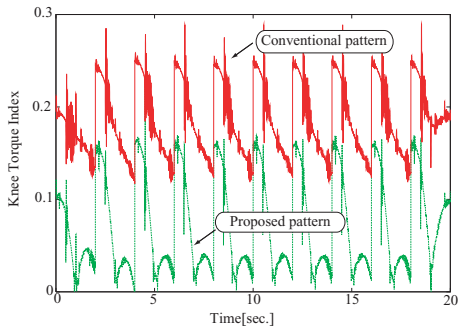

Figure 16: Comparison of Knee Torque Index

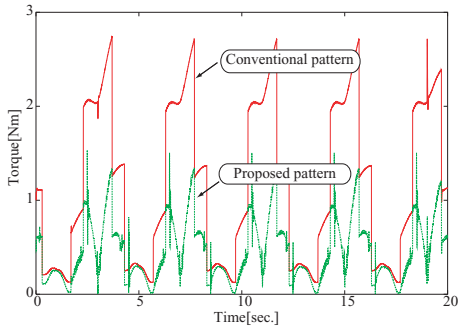

Figure 17: Torque at knee joint of right leg (absolute value)

Computer simulations and experiments are successfully carried out using the humanoid-type proactive interface robot, PICO-2.

Acknowledgments

This research was partly supported by the 21st Century COE Program "Reconstruction of Social Infrastructure Related to Information Science and Electrical Engineering", and the Ministry of Public Management, Home Affairs, Posts and Telecommunications in Japan under Strategic Information and Communications R&D Promotion Programme (SCOPE).

References

[1] A. Takanishi, M. Ishida, Y. Yamazaki, and I. Kato, "The realization of dynamic walking robot wl-10rd," in *Proc. Int. Conf. Advanced Robotics*, 1985, pp. 459–466.

[2] S. Lohmeier, K. Loffler, M. Gienger, H. Ulbrich, and F. Pfeiffer, "Computer system and control of biped "johnnie"," in *IEEE Int. Conf. on Robotics and Automation*, 2004, pp. 4222–4227.

[3] R. Kurazume, S. Tanaka, M. Yamashita, T. Hasegawa, and K. Yoneda, "Straight legged walking of a biped robot," in *2005 IEEE/RSJ International Conference on Intelligent Robots and Systems (IROS)*, 2005, pp. 3095–3101.

[4] R. Kurazume, T. Hasegawa, and K. Yoneda, "The sway compensation trajectory for a biped robot," in *IEEE Int. Conf. on Robotics and Automation*, 2003, pp. 925–931.

[5] R. GARAGE, *CHROINO*. http://www.eonet.ne.jp/ robo-garage/english/frame.html, 2004.

[6] Y. Ogura, H. Akikawa, H. ok Lim, and A. Takanishi, "Realization of strech walking by biped robot (in japanese)," in *Proc of Robotics Symposia*, 2004, pp. 102–107.

[7] ——, "Development of a human-like walking robot having two 7-dof legs and a 2-dof waist," in *IEEE Int. Conf. on Robotics and Automation*, 2004, pp. 134–139.

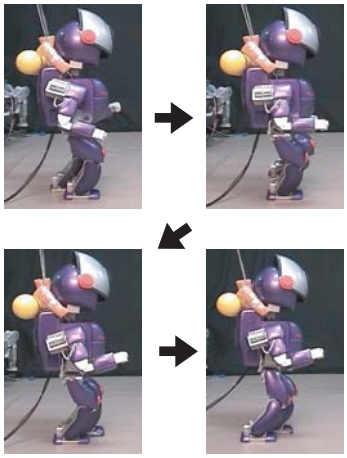

Figure 18: Obtained walking pattern using a conventional walking pattern

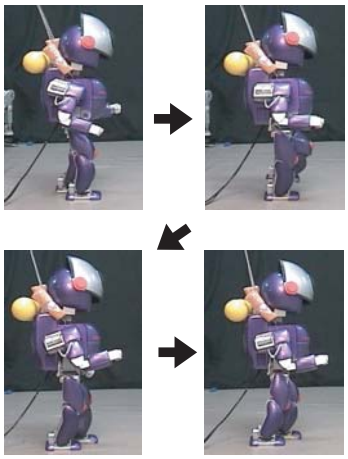

Figure 19: Obtained walking pattern using the proposed method